



Collapse Risk Assessment of Mid-Rise to
High-Rise Buildings with SMRF Equipped with
Viscous Damper (VD) and Buckling-Restrained
Brace Frame (BRBF)

Seyed Arman Hosseini and Mehdi Banazadeh

EasyChair preprints are intended for rapid
dissemination of research results and are
integrated with the rest of EasyChair.

May 27, 2021



COLLAPSE RISK ASSESSMENT OF MID-RISE TO HIGH-RISE BUILDINGS WITH SMRF EQUIPPED WITH VISCOUS DAMPER (VD) AND BUCKLING-RESTRAINED BRACE FRAME (BRBF)

Hosseini, Seyed Arman^{1,3}, Banazadeh, Mehdi²

¹ Research Assistant at Amirkabir University of Technology, Tehran, Iran

² Associate Professor at Amirkabir University of Technology, Tehran, Iran

³ armanhosseinihg@gmail.com

ABSTRACT

In this paper, the seismic collapse risk of mid-rise to high-rise steel frame buildings with the special moment-resisting frame (SMRF) equipped with linear viscous damper (VD) and buckling-restrained braced frame (BRBF) is investigated to compare the seismic performance of both structural systems with different energy-dissipative mechanisms. The buildings studied in this research include 10, 20, and 30-story models with SMRF-VD and BRBF-SMRF systems which are designed according to ASCE7-10 and using ETABS2016 software. In addition, the nonlinear equivalent planner (2D) models of buildings are developed in OpenSees and the collapse fragility curves of each building are obtained based on the results of incremental dynamic analysis (IDA). The panel zone of the SMRF system is modeled by incorporating Joint2D element and modified Ibarra–Medina–Krawinkler (IMK) deterioration model with bilinear hysteresis response assigned to the plastic hinges of SMRF members by using uniaxialMaterial_Bilin material. In addition, for modeling dampers, element_twoNodeLink is used as an element, and uniaxialMaterial_ViscousDamper is incorporated as material in OpenSees. Also, element_truss is utilized for modeling the BRBs, and nonlinear behavior of BRBs are modeled by utilizing uniaxialMaterial_Steel04 and a leaning column is attached to the combined systems to account for the P- Δ effects by rigid beams modeled by utilizing element_truss with considerable axial stiffness. As a conclusion, the 50-year period collapse risk of the buildings has been evaluated and results indicate that the collapse risk of 10, 20, and 30-story BRBF-SMRF buildings are 23.4%, 17.2%, and 14.8% lower compared to SMRF-VD buildings with identical height respectively.

1. INTRODUCTION

Nowadays, mid-rise and high-rise buildings play a vital eco-social role in metropolitan areas. The performance and resilience of these structures under severe earthquake events are significantly crucial. Damage caused by 2011 Canterbury earthquake well highlighted the impact of poor seismic performance of mid-rise and high-rise buildings on business continuity in the downtown area with a high density of these types of buildings (Molina Hutt et al. 2016). An applied method to mitigate the seismic collapse risk of buildings is the use of supplemental damping and structural control systems which can effectively dissipate the earthquake-induced energy and control inelastic deformation and damages in structural members (Bertero and Bertero 2002; Zaker Esteghamati and Farzampour 2020).

The fluid viscous damper (VFD) is a fast-growing passive energy-dissipation mechanism that is currently used in many mid-rise and high-rise buildings to absorb the earthquake-induced energy for seismic design and upgrading purposes. According to experimental and analytical studies conducted by (Dong, Sause and

Ricles 2016), the structural use of viscous dampers can improve the seismic performance of structures as a result of reducing the motion amplitude, inter-story drifts, and absolute accelerations generated by earthquake motions. The ASCE7-10 Standard summarizes design strategies for structures with supplemental passive damping systems. It permits the use of a decreased design base shear force for the seismic design of structures with passive damper where the required performance is similar to or higher than that of the structures with a conventional lateral force-resisting system (ASCE 2013). In addition, significant studies and methods were undertaken to overcome the buckling of brace members in braced-frames due to the beneficial characteristics of this force-resisting system. So, after the introduction of buckling-restrained brace (BRB) and its application as a structural member in Japan, due to its satisfactory hysteresis behavior under cyclic loading, buckling-restrained brace frames (BRBFs) have been used extensively in seismic-resistant structures. In recent years, BRBs have been extensively used in high-rise buildings, serving as energy-dissipating members under severe earthquakes (Marshall 2015).

A BRB member is commonly composed of a steel core encased by the external restraining system. The steel core of a BRB carries the axial load transmitted from adjacent beams and columns of the frame structure, while the external restraining system restrains the lateral deformation of the steel core to prevent it from overall buckling under compression. The key to the mechanism is the axial load going through the steel core while sufficient buckling resistance (flexural rigidity) is provided in another component (Black, Makris and Aiken 2004). In conventional BRBs, the core steel element has a cross-section designed to yield in tension and compression. For this purpose, sufficient flexural rigidity must be provided so the overall buckling load of the composite device is greater than the ultimate strength of the steel core (Guo et al. 2017). The buckling-restrained braced frame (BRBF) was included in the version of ASCE/SEI 7 which was released in 2005, Minimum Standard for Design Loads for Buildings and Other Structures, as an acceptable seismic force-resisting system (ASCE 2013).

In this research, nonlinear equivalent planner (2D) models of the mid-rise to high-rise steel frame buildings with 10, 20, and 30-story with the main structural lateral load resisting system of special moment-resisting frame (SMRF) equipped with linear viscous damper (VD) and the buckling-restrained braced frame (BRBF) have been modeled in OpenSees and the collapse fragility curves of all modeled buildings have been obtained by incorporating the result of incremental dynamic analysis (IDA). Finally, the 50-year period collapse risk of the buildings has been evaluated and compared through the integration of seismic hazard and fragility curves in which the derivative of the fragility curve is combined with hazard curve using the risk integral method.

2. BUILDING DESIGN CRITERIA

In this study, 6 steel mid-rise to high-rise buildings were modeled with 10, 20, and 30 stories and two different lateral load-resisting systems including the special moment-resisting frame (SMRF) equipped with linear viscous damper (VD) which is called SMRF-VD and (SMRF) with buckling-restrained braced frame (BRBF) which is referred to as BRBF-SMRF in this paper.

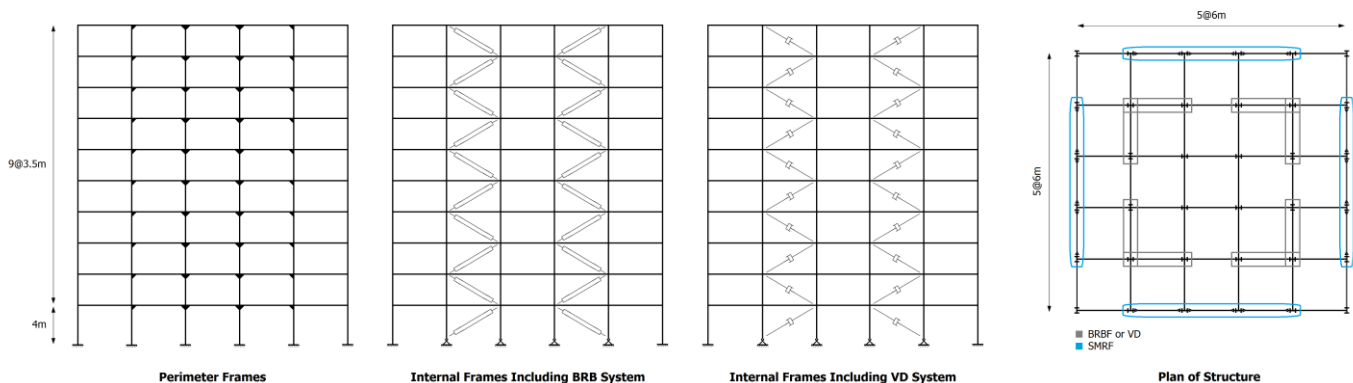


Fig. 1. Plan and elevation view of perimeter and internal frames for 10-story building with both structural systems.

As shown in Fig. 1, only perimeter frames were SMRF, only three middle spans were SMRF in the perimeter frames, and all the beam-to-column joints of the inner members, which were under gravitational loading, were pinned. Furthermore, viscous dampers (VDs) and buckling-restrained braces (BRBs) are located in the internal frame with diagonal installation scheme as are schematically presented in Figure 1 for 10-story structure and for other models with 20-story and 30-story are identical. Also, the buildings were regular and symmetric, all the floors were assumed to act as the rigid diaphragm, the span length is 6 m, and each story has a constant height equal to 3.5 m except that the first floor which has a height equal to 4 m. In order to design the members of both structural lateral load resisting systems and seismic considerations, AISC 360 and AISC 341 codes were used, respectively (FEMA-450 2003; Hwang et al. 2008).

Furthermore, ASCE 7–10 was used for seismic loading and design coefficients (Table 1). In addition, Chapter 18 of ASCE 7–10 was used to design the structures with a damper. Also, steel material was taken as ST52 ($F_y = 3500 \text{ kg/cm}^2$) for structural members except for BRB members which were taken as ST37 with yield strength equal to 2400 kg/cm^2 . Site specifications were extracted from USGS website introduced by ASCE 7–10 and were from San Francisco, The USA, and the soil is considered as Site Class D with the details given in Table 2 (ASCE 2013).

Table 1: Site specifications.

Seismic Force-Resisting System	Response Modification Coefficient, R	Over-strength Factor, Ω_0	Deflection Amplification Factor, C_d
BUILDING FRAME SYSTEMS			
Steel Special Moment Resisting Frame	8	3	5.5
DUAL SYSTEMS WITH SPECIAL MOMENT FRAMES CAPABLE OF RESISTING AT LEAST 25% OF PRESCRIBED SEISMIC FORCES			
Steel Buckling-Restrained Braced Frames	8	2.5	5

Table 2: Design coefficients and factors for seismic-force-resisting systems (ASCE 2013).

Location: San Francisco, CA	Latitude: -122.42 Longitude: 37.78	Calculated Coefficient	
		S_Ds	S_{D1}
0.2 Sec Spectral Acceleration, S_s	1.5412	1.0275	0.6616
1.0 Sec Spectral Acceleration, S_1	0.6616		
Long-Period Transition Period, T_L	8		
Site Coefficient, F_a	1		
Site Coefficient, F_v	1.5		

2.1. Building with SMRF-VD Lateral Load-Resisting System

According to ASCE/SEI-7 standard (ASCE 2013) chapter 18, to design the primary lateral force-resisting system of a structure with supplemental dampers, we can reduce the design base shear force to 75% of the design base shear of a conventional system without dampers. In ASCE 7–10, the structures with a height greater than 30m should be analyzed using the modal response spectrum analysis (MRSA) procedure. In this study, the height of all structures was greater than 30m; therefore, modal response spectrum analysis (MRSA) was applied. First, the un-damped structures are designed for base shear recommended by conventional seismic code without considering drift limitation. Then, the additional viscous damping ratios (β_{v1}) for the selected structures are calculated by MRSA procedure to limit maximum inter-story drift ratio to the allowable values at DBE level equal to 2%. The structural elements and damping system are controlled and possibly redesigned until converging to the target value. To calculate the damping coefficient (C), the equation which is given by (Hwang et al. 2008), was used. In this

study, the expected damping ratio for 10 and 20 story structures was assumed 20%, which was assumed 15% for the structures with 30 stories including the inherent damping ratio of 5%.

The beam and column steel sections of SMRF-VD buildings with 10, 20 and 30 stories and also the damping coefficient of each damper device is listed in Table 3. Because of the symmetry in both directions and lack of common elements between SMRFs in the two directions, the behavior is considered 2-D.

Table 3. Beam and column sections and supplemental damping devices properties of SMRF-VD buildings.

SMRF-VD 10-Story		SMRF			Gravity Frame		
Story Number	Beams	Corner Columns	Middle Columns	Beams	Corner Columns	Middle Columns	
1-5	W24×192	W14×311	W14×426	W16×89	W14×176	W14×176	
6-8	W24×131	W14×211	W14×311	W16×89	W12×106	W12×106	
9-10	W24×76	W14×132	W14×311	W16×89	W12×96	W12×96	
$C_{damper} (kN \cdot sec/m) = 9063.5$, $K_{damper} (kN/m) = 18680367.1$, $\alpha = 1$							
SMRF-VD 20-Story		SMRF			Gravity Frame		
Story Number	Beams	Corner Columns	Middle Columns	Beams	Corner Columns	Middle Columns	
1-5	W24×279	W14×730	W14×730	W16×100	W14×283	W14×283	
6-8	W24×279	W14×550	W14×605	W16×100	W14×193	W14×193	
9-10	W24×279	W14×426	W14×605	W16×100	W14×176	W14×176	
11-15	W24×207	W14×370	W14×500	W16×100	W14×145	W14×145	
16-20	W24×192	W14×311	W14×426	W16×100	W14×82	W14×82	
$C_{damper} (kN \cdot sec/m) = 12565.8$, $K_{damper} (kN/m) = 15325953.1$, $\alpha = 1$							
SMRF-VD 30-Story		SMRF			Gravity Frame		
Story Number	Beams	Corner Columns	Middle Columns	Beams	Corner Columns	Middle Columns	
1-6	W27×307	W18×1525	W14×730	W16×100	W14×605	W14×605	
7-8	W27×307	W16×1185	W14×730	W16×100	W14×398	W14×398	
9-12	W27×307	W15×1035	W14×730	W16×100	W14×342	W14×342	
13-20	W27×281	W14×730	W14×730	W16×100	W14×193	W14×193	
21-25	W27×194	W14×455	W14×550	W16×100	W14×132	W14×132	
$C_{damper} (kN \cdot sec/m) = 24458.5$, $K_{damper} (kN/m) = 26256283.6$, $\alpha = 1$							

2.2. Building with BRBF-SMRF Lateral Load-Resisting System

Design provisions for BRBFs in the United States exist since 2005 and are included in Minimum Design Loads for Buildings and Other Structures, ASCE7-10 and the Seismic Provisions for Structural Steel Buildings, AISC341-10. Specific design provisions for BRBFs are given in AISC 341-10, Section F4. Essentially, these provisions aim to result in a BRBF design that is able to present significant inelastic deformation capacity mainly through brace yielding in tension and compression. To achieve this, braces shall be designed, detailed and tested to accommodate expected deformations. Expected deformations correspond to the maximum between 2% story drift and two times the design story drift. The steel core is designed to resist the total axial load in the brace and its design axial strength $\phi F_{y_{sc}} \times A_{sc}$ where ϕ is equal to 0.9, $F_{y_{sc}}$ is specified minimum yield stress of the core, or actual yield stress of the steel core determined from a coupon test in Mpa, and A_{sc} is cross-sectional area of the yielding segment of the steel core in mm².

For the analysis, braces are not considered to resist gravity loading, and the required strength of beams, columns, and connections shall be based on the applicable load combinations that include the amplified seismic load coming from the adjusted brace strength in tension and compression, as it is presented in Fig. 2 where β is compression strength adjustment factor, ω is strain hardening adjustment factor and R_y is ratio of expected yield stress to the specified minimum yield stress, it does not need to be applied if $P_{y_{sc}}$ is determined from a coupon test. These adjustment factors are determined from the qualification tests specified in Section K3.4c of the Seismic Provisions. Where β is the ratio of the maximum compression force, P_{max} to the maximum tension force, T_{max} and ω is the ratio of the maximum tension force, T_{max} to the

measured yield force, $R_y P_{y,sc}$. Due to the test configuration, these maximums occur at $2.0\Delta_{bm}$, where Δ_{bm} is the design story drift, as shown in Fig. 2. Finally, beams and columns shall satisfy the requirements for highly ductile members.

In addition, ASCE7-10 includes Dual Systems, consisting of a BRBF and a SMRF, as an option for Seismic Force-Resisting Systems (SFRS). The first prototype design for dual systems was based on the ASCE7-10 requirement, the BRBF was proportioned to resist the full design base shear and the SMRF was sized for 25 percent of the design seismic forces applied to the BRBF. Modal response spectrum analysis (MRSA) was also used for the design of dual systems and the BRBF designs still included P- Δ effects. The SMRF design was performed in accordance with AISC Seismic Provisions. The beam and column steel sections of BRBF-SMRF buildings with 10, 20 and 30 stories and also the BRB members are listed in Table 4.

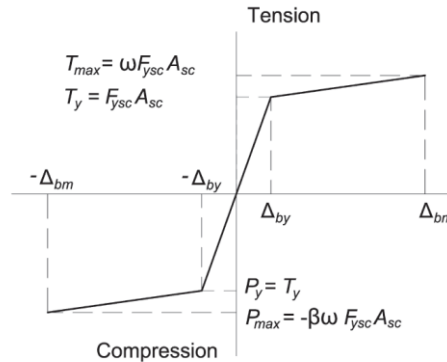


Figure 2. Diagram of brace force-displacement (Adapted from AISC 2010).

Table 4. Beam, column and BRB sections of BRBF-SMRF buildings.

BRBF-SMRF 10-Story		SMRF			BRBF		
Story Number	Beams	Corner Columns	Middle Columns	Beams	Columns	BRB	
1	W16x57	W14x132	W14x132	W16x89	W14x370	StarBRB_18.0	
2-3	W16x57	W14x132	W14x132	W16x89	W14x342	StarBRB_14.0	
4	W16x57	W14x132	W14x132	W16x89	W14x211	StarBRB_14.0	
5-7	W16x40	W12x96	W12x96	W16x89	W14x176	StarBRB_12.0	
7	W16x40	W12x96	W12x96	W16x89	W14x145	StarBRB_12.0	
8-10	W16x40	W12x96	W12x96	W16x89	W14x370	StarBRB_18.0	
BRBF-SMRF 20-Story		SMRF			BRBF		
Story Number	Beams	Corner Columns	Middle Columns	Beams	Columns	BRB	
1-3	W18x158	W14x342	W14x342	W16x100	W15x1035	StarBRB_23.0	
4-5	W18x158	W14x342	W14x342	W16x100	W14x730	StarBRB_18.0	
6-9	W18x158	W14x311	W14x311	W16x100	W14x605	StarBRB_18.0	
10-12	W18x130	W14x233	W14x233	W16x100	W14x426	StarBRB_16.0	
13-15	W18x130	W14x233	W14x233	W16x100	W14x283	StarBRB_12.0	
16-18	W18x97	W14x176	W14x176	W16x100	W14x132	StarBRB_8.0	
19-20	W18x97	W14x176	W14x176	W16x100	W14x74	StarBRB_8.0	
BRBF-SMRF 30-Story		SMRF			BRBF		
Story Number	Beams	Corner Columns	Middle Columns	Beams	Columns	BRB	
1-3	W18x192	W14x605	W14x605	W16x100	W15x1035	StarBRB_30.0	
4-5	W18x192	W14x550	W14x550	W16x100	W14x770	StarBRB_30.0	
6-7	W18x192	W14x550	W14x550	W16x100	W14x730	StarBRB_30.0	
8-11	W18x192	W14x426	W14x426	W16x100	W14x605	StarBRB_24.0	
12-13	W18x175	W14x370	W14x370	W16x100	W14x500	StarBRB_24.0	
14-15	W18x175	W14x370	W14x370	W16x100	W14x455	StarBRB_20.0	
16-17	W18x175	W14x342	W14x342	W16x100	W14x398	StarBRB_20.0	

18-19	W18×175	W14×342	W14×342	W16×100	W14×342	StarBRB_16.0
20-24	W14×257	W18×106	W14×257	W16×100	W14×283	StarBRB_14.0
25-30	W14×211	W18×106	W14×211	W16×100	W14×159	StarBRB_12.0

3. ANALYTICAL MODEL DEVELOPMENT

Fig. 3 and Fig. 4 shows analytical nonlinear models of developed two-dimensional (2D) of the SMRF-VD and BRBF-SMRF in the East-West direction which were developed in OpenSees (McKenna 2011). Effect of nonlinearity in both material and geometry were included in the FE code. Geometry and material nonlinearity of SMRF was implemented by utilizing P-Delta transformation and simulating plastic hinges at the ends of each beam-column element, respectively. Modified Ibarra–Medina–Krawinkler (IMK) deterioration model with bilinear hysteresis response was assigned to the plastic hinges of SMRF members by using uniaxialMaterial_Bilin material in OpenSees (Ibarra, Medina and Krawinkler 2005).

In addition, the panel zone is modeled by incorporating Joint2D element in OpenSees by assigning a rigid material as shear panel behavior and the connected column and beam depths are used as the width and height of the panel zone element, respectively as demonstrated in Fig. 3 and Fig. 4. In Addition, beam and column members of SMRF which are located between plastic hinges were modeled with elasticBeamColumn elements in OpenSees with Steel02 material. A leaning column is attached to the combined Seismic Force-Resisting Systems (SFRS) to account for the P-Δ effects by rigid beams which are modeled by utilizing element_truss with considerable axial stiffness in OpenSees. The load carried by the gravity system is applied to the leaning column and the floor mass is uniformly assigned to each joint node. As illustrated in Fig. 3, for modeling supplemental damping devices, element_twoNodeLink is used as an element and for material the developed code by Akcelyan and Lignos as uniaxialMaterial_ViscousDamper is incorporated in OpenSees by inputting elastic stiffness of linear spring to model the axial flexibility of a viscous damper (combined stiffness of the supporting brace and internal damper portion) K_{damper} , damping coefficient C_{damper} , and velocity exponent α as supplemental damping devices properties (Akcelyan et al. 2016).

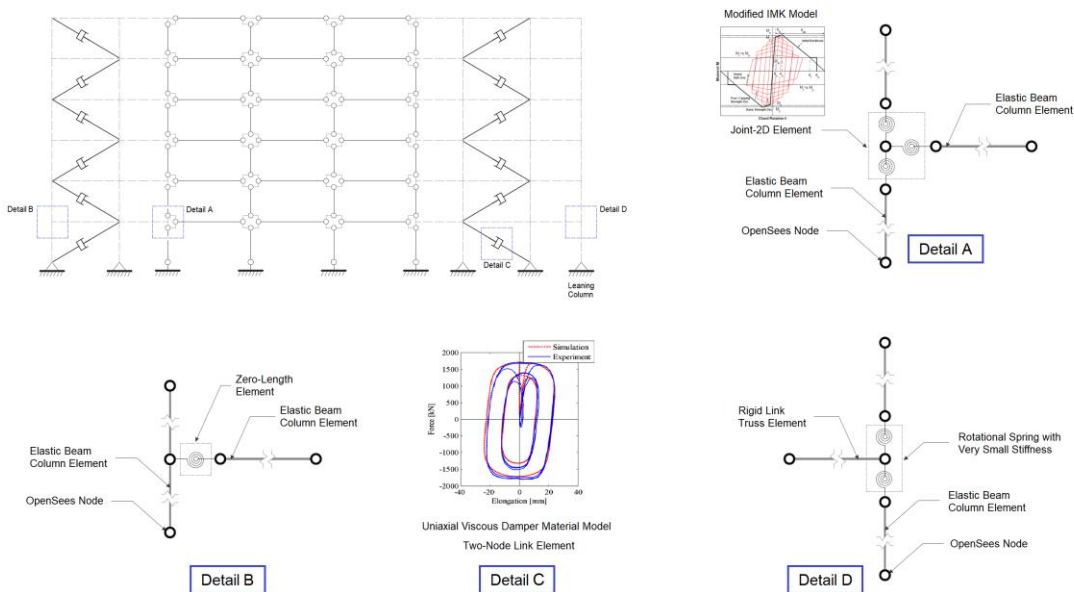


Fig. 3. Schematic illustration of analytical modeling of SMRF-VD in OpenSees.

Also, the purpose of utilizing BRBs is to prevent the buckling phenomenon which would be usually provided by an outer steel restraining tube supporting the yielding steel core. As a result, element_truss is utilized for modeling the BRBs because it cannot buckle and there is no need to model the outer steel restraining

tube be since its effect is indirectly intended. To model the whole BRB, it is sufficient to incorporate the `element_truss` command and assign the cross-section and specifications of the steel yielding core to the element. The nonlinear behavior of BRBs are modeled by utilizing `uniaxialMaterial_Steel04` which have recently been introduced by Zsarnóczy as material (Zsarnóczy and Vigh 2017). Finally, the BRBF and damping system consists of a couple of one-bay frames are connected to both sides of the SMRF by rigid beams pinned at both ends respectively to complete two-dimensional (2D) models of the SMRF-VD and BRBF-SMRF buildings (Safaei et al. 2019).

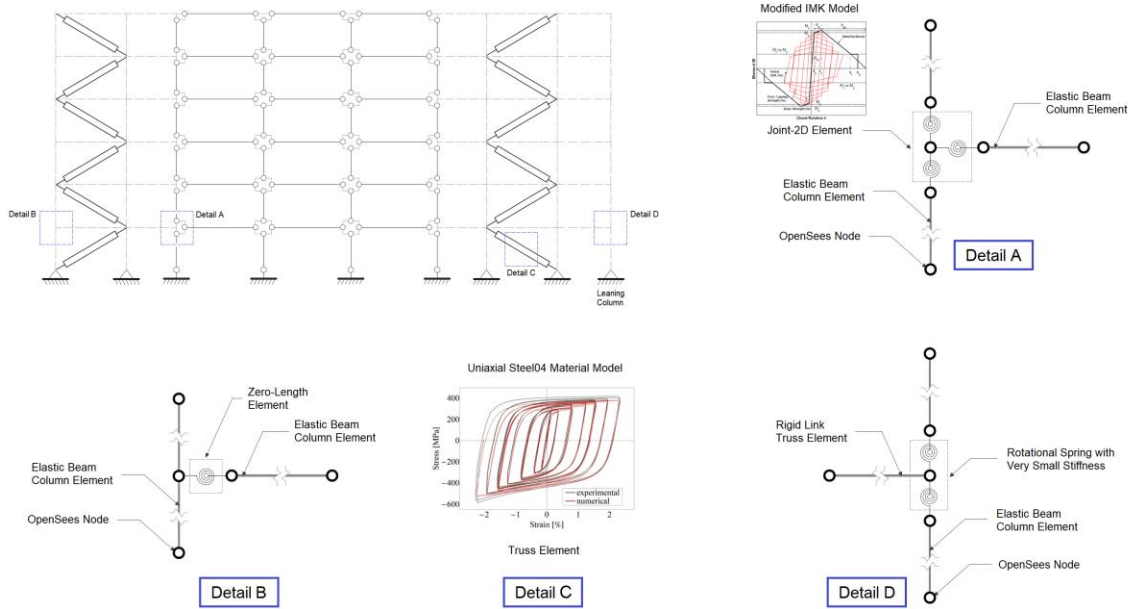


Fig. 4. Schematic illustration of analytical modeling of BRBF-SMRF in OpenSees.

4. INCREMENTAL DYNAMIC ANALYSIS (IDA)

The seismic performance of the SMRF-VD and BRBF-SMRF models is assessed utilizing incremental dynamic analysis (IDA) (Vamvatsikos and Cornell 2002). IDA is a method in which the intensity measure (IM) value is systematically increased from a small initial quantity until the damage measure (DM) value exceeds to the point where the model collapses under the lateral seismic forces. The “Hunt and Fill” algorithm was incorporate for this process (Vamvatsikos 2011). For performing an IDA, one of the most crucial considerations is to choose an appropriate intensity measure (IM) and damage measure (DM). In this study, 5% damped first mode spectral acceleration, $S_a[T_1]$ and maximum inter-story drift ratio, θ_{max} were chosen as IM and DM, respectively. During the IDAs, collapse is taken as the point at which the IDA curve slope reduced to 20% of the elastic slope, dynamic instability occurs or a drift limit of 10% for SMRF-VD and BRBF-SMRF models is exceeded. This assumption is consistent with Table 4–10 of the SAC report, which states that collapse prevention performance is broken when the story drift exceeds 10% (Lignos and Krawinkler 2013).

The set of 44 (22 pairs) far-field ground motion records specified in FEMA P695 are used. The magnitude for these records varies from M6.5 to M7.6 with an average of M7.0. Thirty-two (16 pairs) of the ground motions were recorded at sites classified as site class D and the remaining records are from site class C locations. The peak ground acceleration for the record set varies from 0.21g to 0.82g with an average of 0.43g. More detailed information about the ground motion records can be found in Appendix of FEMA P695. Scaling for IDAs is performed such that the median spectral acceleration of the record set matches the specified intensity levels, which ranges from 0.2g to 3.0g (FEMA P58-1. 2012). The results of IDA curves for the 10, 20, and 30-story SMRF-VD and BRBF-SMRF models are shown in Fig. 5.

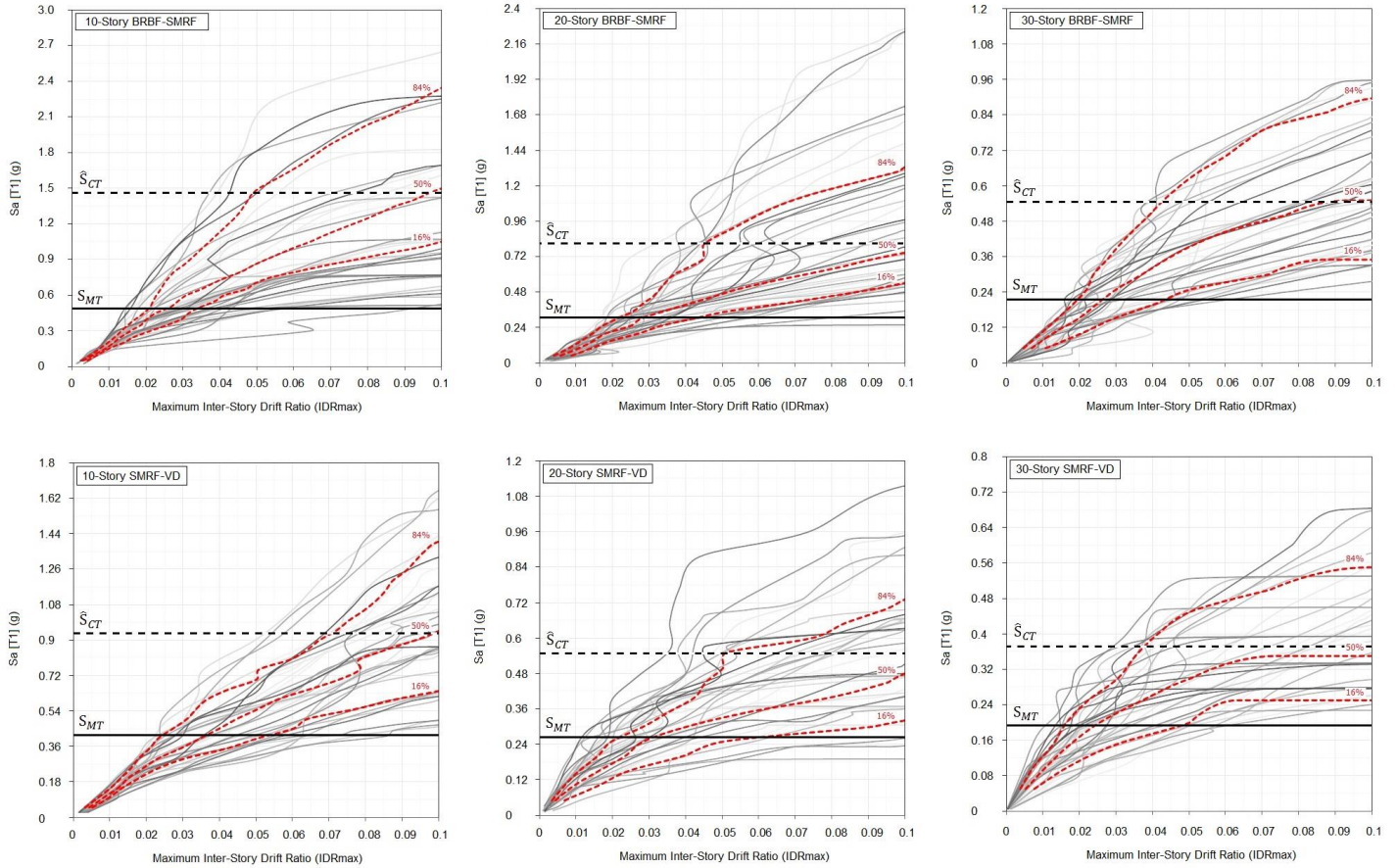


Fig. 5. IDA curves for the 10, 20, and 30-story SMRF-VD and BRBF-SMRF models.

5. FRAGILITY CURVES AND RISK ASSESSMENT OF STRUCTURES

The IDA results are used to obtain fragilities for the SMRF-VD and BRBF-SMRF models. Fragility functions are used to quantify the probability that the structure will exceed a particular damage state as a function of some intensity measure (IM). In this study, the probability of collapse on the spectral acceleration level at the 1st mode period is determined from the IDA results. The fragility curve is a cumulative distribution function of median collapse spectral acceleration from individual records. The collapse fragility curve is assumed to follow approximately a cumulative lognormal distribution (Vamvatsikos and Cornell 2002; Bradley and Dhakal 2008).

Fig. 5 shows the collapse fragility curves for the 10, 20, and 30-story SMRF-VD and BRBF-SMRF buildings. As expected, by increasing the height of buildings and subsequently increasing the P- Δ effect under far-field earthquakes, the probability of collapse raised. In the comparison between the structures with SMRF-VD and BRBF-SMRF, the probability of collapse was smaller in the structures with dual systems than the structures with supplemental damping systems.

Although, the 50-year collapse risk of structures with both Seismic Force-Resisting Systems (SFRS) has been calculated through the integration of seismic hazard and fragility curves in which the derivative of fragility curve is combined with hazard curve using the risk integral (Judd and Charney 2014). According to Fig. 7, The results indicated that the 50-year collapse risk for the 10, 20, and 30-story models with BRBF-SMRF system is equal to 2.25%, 6.15%, and 10.24% respectively. However, this ratio is about 2.94%, 7.43%, and 12.02% for 10, 20, and 30-story models with SMRF-VD system.

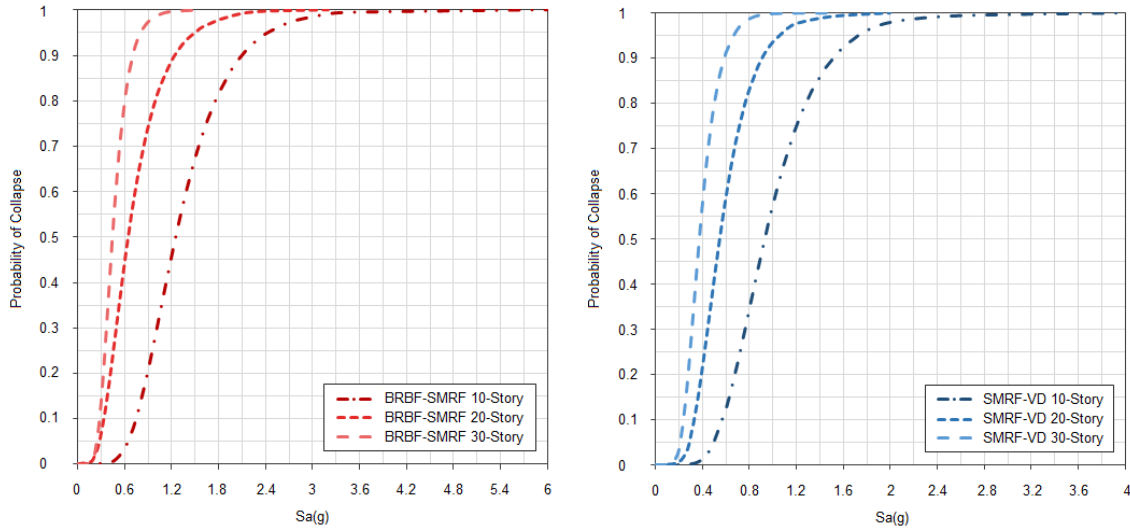


Fig. 6. Collapse fragility curves for the 10, 20, and 30-story SMRF-VD and BRBF-SMRF models.

6. CONCLUSION

A comparative assessment of the collapse risk for the 10, 20, and 30-story SMRF-VD and BRBF-SMRF is presented. Firstly, analytical models of designed 10, 20, and 30-story office buildings with both Seismic Force-Resisting Systems (SFRS) were developed in OpenSees. Secondly, incremental dynamic analysis (IDA) was performed to study the response of the modeled buildings. Based on the results which are shown in Fig. 7 it can be concluded that the collapse risk of buildings with higher height is considerably greater than that of the building with a lower height. More specifically, the 50-year collapse risk of 10, 20, and 30-story BRBF-SMRF buildings are 23.4%, 17.2%, and 14.8% lower compared to SMRF-VD buildings with identical height respectively. As a result, it can be inferred that the seismic performance of BRBF-SMRF dual system toward controlling the collapse risk is more superior compared to SMRF-VD system. However, the collapse risk of both systems gets more close together by increasing the height of buildings.

$$\begin{aligned}
 \lambda_F &= -\int_0^{+\infty} u dv \\
 &= -[uv]_0^{+\infty} - \int_0^{+\infty} v du \\
 &= -[P(F|a) \lambda_a]_0^{+\infty} + \int_0^{+\infty} \lambda_a f(a) da \\
 &= -[P(F|a) \lambda_a]_0^{+\infty} + \int_0^{+\infty} \lambda_a f(a) da \\
 &= -[(1)(0) - (0)(1)] + \int_0^{+\infty} \lambda_a f(a) da \\
 &= \int_0^{+\infty} \lambda_a f(a) da
 \end{aligned}$$

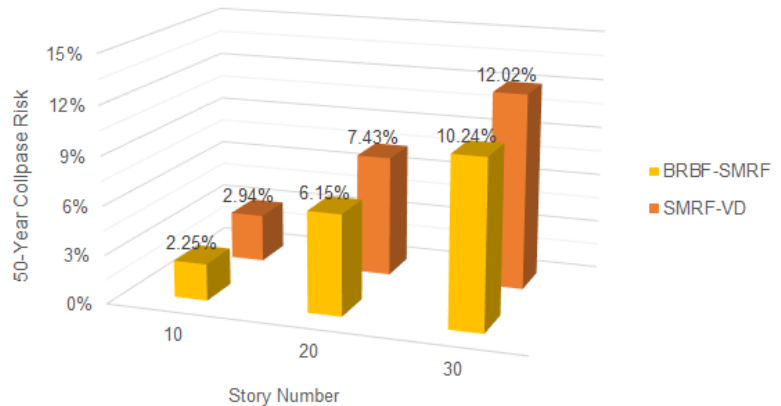


Fig. 7. Comparison of 50-year collapse risk for the 10, 20, and 30-story models with SMRF-VD and BRBF-SMRF systems based on derivative of fragility curve method (Judd and Charney 2014).

REFERENCES

American Society of Civil Engineers & American Society of Civil Engineers. (2013). "Minimum Design Loads for Buildings and Other Structures". *American Society of Civil Engineers*.

Akcelyan, Sarven, Dimitrios G. Lignos, Tsuyoshi Hikino, and Masayoshi Nakashima. 2016. "Evaluation of Simplified and State-Of-The-Art Analysis Procedures for Steel Frame Buildings Equipped with

- Supplemental Damping Devices Based On E-Defense Full-Scale Shake Table Tests". *Journal of Structural Engineering* 142 (6): 04016024. doi:10.1061/(asce)st.1943-541x.0001474.
- Bertero, Raul D., and Vitelmo V. Bertero. 2002. "Performance-Based Seismic Engineering: The Need for A Reliable Conceptual Comprehensive Approach". *Earthquake Engineering & Structural Dynamics* 31 (3): 627-652. doi:10.1002/eqe.146.
- Black, Cameron J., Nicos Makris, and Ian D. Aiken. 2004. "Component Testing, Seismic Evaluation and Characterization of Buckling-Restrained Braces". *Journal of Structural Engineering* 130 (6): 880-894. doi:10.1061/(asce)0733-9445(2004)130:6(880).
- Bradley, Brendon A., and Rajesh P. Dhakal. 2008. "Error Estimation of Closed-Form Solution for Annual Rate of Structural Collapse". *Earthquake Engineering & Structural Dynamics* 37 (15): 1721-1737. doi:10.1002/eqe.833.
- Dong, Baiping, Richard Sause, and James M. Ricles. 2016. "Seismic Response and Performance of a Steel MRF Building with Nonlinear Viscous Dampers Under DBE and MCE". *Journal of Structural Engineering* 142 (6): 04016023. doi:10.1061/(asce)st.1943-541x.0001482.
- FEMA 450. (2003). *NEHRP Recommended Provisions for Seismic Regulations for New Buildings and Other Structures*. Federal Emergency Management Agency.
- FEMA P58-1. 2012. "Seismic Performance Assessment of Buildings". *Applied Technology Council, Redwood City, CA*.
- Guo, Yan-Lin, Jing-Zhong Tong, Xiao-An Wang, and Bo-Hao Zhang. 2017. "Subassemblage Tests and Numerical Analyses of Buckling-Restrained Braces Under Pre-Compression". *Engineering Structures* 138: 473-489. doi:10.1016/j.engstruct.2017.02.046.
- Hwang, Jenn-Shin, Yin-Nan Huang, Shy-Lian Yi, and Song-Yen Ho. 2008. "Design Formulations for Supplemental Viscous Dampers to Building Structures". *Journal of Structural Engineering* 134 (1): 22-31. doi:10.1061/(asce)0733-9445(2008)134:1(22).
- Ibarra, Luis F., Ricardo A. Medina, and Helmut Krawinkler. 2005. "Hysteretic Models That Incorporate Strength and Stiffness Deterioration". *Earthquake Engineering & Structural Dynamics* 34 (12): 1489-1511. doi:10.1002/eqe.495.
- Judd, J.P. and Charney, F.A. 2014. "Earthquake Risk Analysis of Structures". *Proceedings of the 9th International Conference on Structural Dynamics*. EUROODYN, 2929-2938.
- Lignos, D and Krawinkler, H. 2013. "Sidesway Collapse of Deteriorating Structural Systems Under Seismic Excitations". *John A. Blume Earthquake Engineering Center Technical Report 177*. Stanford Digital Repository. Available at: <http://purl.stanford.edu/yg701cw5473>.
- Marshall, Justin D. 2015. "Buckling-Restrained Braces and Their Implementation in Structural Design of Steel Buildings". *Encyclopedia of Earthquake Engineering*, 1-11. doi:10.1007/978-3-642-36197-5_313-1.
- McKenna, Frank. 2011. "Opensees: A Framework for Earthquake Engineering Simulation". *Computing in Science & Engineering* 13 (4): 58-66. doi:10.1109/mcse.2011.66.
- Molina Hutt, Carlos, Ibrahim Almufti, Michael Willford, and Gregory Deierlein. 2016. "Seismic Loss and Downtime Assessment of Existing Tall Steel-Framed Buildings and Strategies for Increased Resilience". *Journal of Structural Engineering* 142 (8). doi:10.1061/(asce)st.1943-541x.0001314.
- Safaei, Shayan, Arsam Taslimi, and Payam Tehrani. 2019. "A Study on the Accuracy of Force Analogy Method in Nonlinear Static Analysis." *The Structural Design of Tall and Special Buildings* 28 (13). doi:10.1002/tal.1654.
- Vamvatsikos, Dimitrios, and C. Allin Cornell. 2002. "Incremental Dynamic Analysis". *Earthquake Engineering & Structural Dynamics* 31 (3): 491-514. doi:10.1002/eqe.141.
- Vamvatsikos, Dimitrios. 2011. "Performing Incremental Dynamic Analysis in Parallel". *Computers & Structures* 89 (1-2): 170-180. doi:10.1016/j.compstruc.2010.08.014.
- Zaker Esteghamati, Mohsen, and Alireza Farzampour. 2020. "Probabilistic Seismic Performance and Loss Evaluation of a Multi-Story Steel Building Equipped with Butterfly-Shaped Fuses." *Journal of Constructional Steel Research* 172: 106187. doi:10.1016/j.jcsr.2020.106187.
- Zsarnóczyay, Ádám, and László Gergely Vigh. 2017. "Eurocode Conforming Design of BRBF – Part II: Design Procedure Evaluation". *Journal of Constructional Steel Research* 135: 253-264. doi:10.1016/j.jcsr.2017.04.013.